Numerical Simulation on Cavitation in a Vane Pump with Moving Mesh

***Qunfeng Zhang[1,2], X.Y. Xu[3]**

[1]School of Civil Engineering, Beijing Jiaotong University, Beijing, 100044, China
[2]Department of Chemical Engineering, Imperial College London, South Kensington Campus, London SW7 2AZ, United Kingdom
[3]Department of Chemical Engineering, Imperial College London, South Kensington Campus, London SW7 2AZ, United Kingdom

*Corresponding author: zhangqunfeng@263.net

Abstract

Cavitation can occur in vane pumps when the local fluid static pressure falls below the vapor pressure at the operating conditions. Cavitation can reduce the flow rate and erode the internal surface of a vane pump. Because direct measurement is difficult to implement, predictive tools based on Computational Fluid Dynamic (CFD) has become a valid alternative approach to determine the position and size of cavitation in a vane pump. In this study, a purpose-built code has been developed for use with Star-CD to capture the gap shape between the vane and stator with a moving mesh. The internal flow of a vane pump has been simulated with the volume of fluid method, together with Rayleigh cavitation model and RANS-based Mender's SST $k-\omega$ turbulence model. The simulation results demonstrate the initiation, development and collapse of cavitation during the rotation of vane, which leads to accumulation or release of the mass of oil, resulting in a reduced or increased area of cavitation respectively. The transient flow rate at the inlet is stable while the outlet flow rate fluctuates significantly. The radiuses of vane tip and gap size are found to influence the size of cavitation and flow rate of the vane pump. The computational model presented here can provide the basis for optimal design of vane pumps.

Keywords: Vane pump, Numerical simulation, Moving mesh, Volume of fluid method, Cavitation model, Turbulence model

Introduction

The physical phenomenon of cavitation can occur in vane pumps when the local fluid static pressure falls below the vapor pressure at the operating conditions. The vane pump operating performance is greatly affected by the cavitation. Usually, the cavitation can reduce the working life, efficiency of vane pump and can generate vibration, noise and solid surface erosion in vane pump. Vane pump cavitation are mainly blade surface cavitation and clearance cavitation. The blade surface cavitation is generated at the position with low static pressure induced by the secondary flow near blade surface while the clearance caviation is generated for the local high speed leakage velocity near the clearance between tip of vane and stator wall. Researchers [Shcherbin and Smolyanskii (1994); Cho and Han (1998);Wu (2005); Antonio and Rosario (2005), L.Wang and Quan (2006)] have utilized theoretical analysis and empirical formulas to investigate the effect factors like profile curve of the stator, flow rate fluctuation of pump, and indicated the important effect factors of the performance and service life of vane pump. In the past, theoretical analysis and empirical formulas have been mainly relied on during the process of pump design, however it is not sufficient. It is important to follow a combined strategy between simulation, experiment and analysis to design a vane pump with the characteristics of large flow rate, high pressure and low noise. Solving the three

dimensional Navier-Stokes equations based on finite volume method plays an important role in predicting the performance of the vane pump.

The key factors of accurately simulating the vane pump internal flow are grid deformation and reconstruction as the chamber volume changes. The selection of cavitation model and turbulence model also plays an important role. The common CFD softwares utilized in the simulation of vane pump flow include FLUENT, Pumplinx and Starccm+, etc. But simplifications were made such as simplifying the geometry and fitting the profile curve of vane tip to the profile curve of stator. Sometimes artificially enlarged leakage gap was performed in order to avoid numerical convergence problems. All these modifications led to less accurate simulations of the leakage and cavitation phenomena of the vane pump.

In this paper, a purpose-built code for the computational fluid dynamics software Star-CD has been completed. This program can generate the grids in the cases of different vanes number, different profile curves of stator or different gap sizes in a fast way. It is especially capable of capturing the gap shape between the vane and the stator. In the present simulation, this feature was used combined with the Menter SST k-ω turbulence model [Menter (1994)], the Rayleigh cavitation model [Ahuja et al (2001); Bakirand Gerber (2004)] and VOF [Hirt and Nichols (1981); Ubbink and Issa (1999)] method. The flow characteristics together with the generation, development and collapse of cavitation were analyzed. Influences of the radius of vane tip on the pump performances were investigated. The comparisons of the computed results are consistent with the experimental data, indicating the appropriate selections of numerical method and models.

Governing Equations and Cavitation Model

To simulate the generation, development and collapse of cavitation in a vane pump, the three dimensional averaged Navier-Stokes equations combined with the VOF method and Rayleigh cavitation model were solved. The governing volume-fraction equations for the vapor and liquid lubricant oil are as follows:

$$\frac{\partial \rho_v \beta}{\partial t} + \frac{\partial \rho_v (u_j - v_{gj})\beta}{\partial x_j} = \rho_v S_\beta \tag{1}$$

$$\frac{\partial \rho_l \alpha}{\partial t} + \frac{\partial \rho_l (u_j - v_{gj})\alpha}{\partial x_j} = -\rho_v S_\beta \tag{2}$$

where α and β are volume fractions of liquid and vapor lubricant oil respectively. The sum of the two volume fractions must satisfy: $\alpha + \beta = 1$ .The source term S_β accounts for mass exchange between the liquid and vapor phases during cavitation generating. ρ_l and ρ_v are densities of liquid and vapor of oil respectively. It is S_β .is calculated from the Rayleigh cavitation model.

The governing momentum equation for the vapor-liquid mixture is:

$$\frac{\partial \rho u_i}{\partial t} + \frac{\partial \rho (u_j - v_{gj}) u_i}{\partial x_j} = -\frac{\partial p}{\partial x_i} + \rho g_i + f + \frac{\partial \tau_{ij}}{\partial x_j} \tag{3}$$

where density ρ is defined through the volume fractions as $\rho = \rho_l \alpha + \rho_g \beta$. f is the source term of momentum transport at the interface between the liquid and vapor phase.

$$\tau_{ij} = 2\mu S_{ij} - \frac{2}{3}\mu \frac{\partial u_k}{\partial x_k}\delta_{ij} - \rho \overline{u_i' u_j'} \qquad S_{ij} = \frac{1}{2}\left(\frac{\partial u_i}{\partial x_j} + \frac{\partial u_j}{\partial x_i}\right) \tag{4}$$

$$\mu = \alpha \mu_l + \beta \mu_v \tag{5}$$

τ_{ij} is the deformation tensor. δ_{ij} is the Kronecker operator. S_{ij} is the deformation rate tensor. And the dynamic viscosity μ is defined through the volume fractions.

Due to the grid deformation and reconstruction during simulation, an additional equation has to be satisfied simultaneously with the other conservation equations. The space conservation law (SCL) [Demirdzic and Peric (1998)] is used to avoid generating artificial mass sources during numerical solution procedure. The conservation equation is described by:

$$\frac{d}{dt}\int_{V_P} dV - \sum_{k=1}^{n_f} \int_{S_k} v_{gj} \cdot dS_j = 0 \tag{6}$$

where v_{gj} is the grid velocity, n_f the number of grid cells on the surface of the control volume, and the surface vector dS_j.

Turbulence Model

The eddy viscosity model is used for the Reynolds stress term to close the equation set.

$$-\rho\overline{u_i' u_j'} = \tau_{tij} = 2\mu_t S_{ij} - \frac{2}{3}(\mu_t \frac{\partial u_k}{\partial x_k} + \rho k)\delta_{ij} \tag{7}$$

where k is the turbulent kinetic energy and μ_t is the turbulent viscosity.

The shear stress transport (SST) k-ω turbulence model is developed by Menter, who used the SST k-ω model often merit it for its good behavior in adverse pressure gradients and separating flow. The SST model can be switched to a k-ε turbulence model in the free-stream and thereby avoids the common k-ω problem that the model is too sensitive to the inlet free-stream turbulence properties.

The turbulence kinetic energy k and the specific dissipation rate ω are obtained from the following transport equations:

$$\frac{\partial}{\partial_t}(\rho k)+\frac{\partial}{\partial x_j}[\rho(u_j - v_{gj})k] = \mu_t P - \rho\beta^* \omega k + \frac{\partial}{\partial x_j}\left[(\mu+\sigma_k\mu_t)\frac{\partial k}{\partial x_j}\right] \tag{6}$$

$$\frac{\partial}{\partial_t}(\rho\omega) + \frac{\partial}{\partial x_j}[\rho(u_j - v_{gj})\omega] = \gamma\rho P - \beta\rho\omega^2 + \frac{\partial}{\partial x_j}\left[(\mu+\sigma_\omega\mu_t)\frac{\partial\omega}{\partial x_j}\right] + (1-F_1)2\rho\sigma_\omega \frac{1}{\omega}\frac{\partial k}{\partial x_j}\frac{\partial\omega}{\partial x_j} \tag{7}$$

$$\mu_t = \rho\frac{k}{\omega} \quad P = S_{ij}\frac{\partial u_i}{\partial x_j} \tag{8}$$

where σ_k, β^*, γ, β, F_1 are the empirical constants obtained from theoretical analysis combined with experimental data.

Grid Generation and Numerical method

Figure 1 is the section structure of the vane pump. The regions without vane rotating have been generated hexahedral grids using the mesh generator software ICEM-CFD while the region with vane rotating has been generated hexahedral grids with a purpose-built code developed by author. The purpose-built code can control the key nodes on the profile curve of the stator, and generate the moving grids by an algebraic grid generation method. So the gaps shape between the vane and stator can be captured well. The total amount of grid cells is about 560,000. Presented in Figure 2 is the grid of the rotating region (chamber), deforming with the rotation of the shaft. The thin layer grids on top surface and bottom surface are the gaps in axial direction. Figure 3 shows the good orthogonal grids near the gap with different radius (R=17mm, 34mm and 51mm) of vane tip. In the

process of calculations, the grids deform at each time step. Grids were generated in the chamber cells at current time step and the three-dimensional coordinates of the nodes were output to a file. Then a commercial finite-volume-based CFD software Star-CD reads coordinate data from the file by subroutine and complete the iteration. The spatial discretization was achieved via a second-order difference scheme MARS (Monotone Advection and Reconstruction Scheme), which based on the TVD scheme. The SIMPLE algorithm is used for the pressure-velocity coupling for the unsteady calculations. In order to improve the convergence rate and stability, a solution based on single-phase without cavitation model is first computed. Then initialized from this non-cavitating solution, the two-phase mixture solutions with activating cavitation model were calculated.

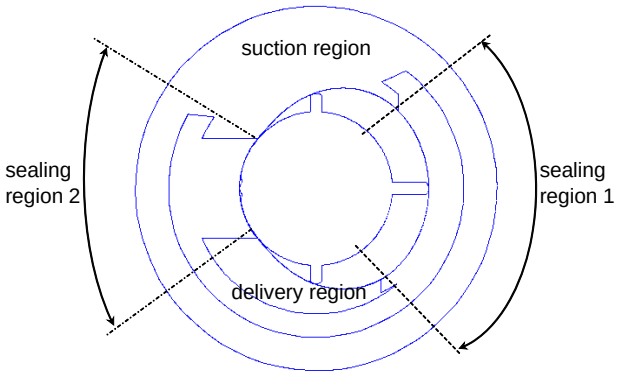

Figure 1 Section structure of vane pump

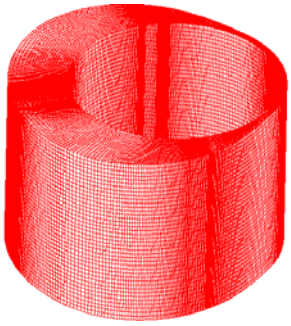

Figure 2 Grid of rotating region

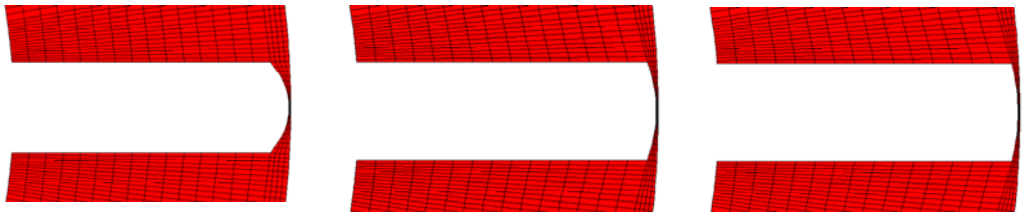

R=17mm R=34mm R=51mm

Figure 3 Grid near the gap with different radius of vane tip

Boundary Condition and Computational Cases

Often the conditions at the boundaries should represent exactly the physical conditions. For the vane pump, inlet and outlet pressure of the pump have fluctuations in reality, and setting variable pressures at inlet and outlet boundaries which needs to be measured by tests is more accurate in computation. But it is difficult to match the transient pressures with the corresponding rotor angle even if the variable pressures are obtained. So a constant values of pressure were specified at the inlet and outlet of the pump. All wall surfaces were set in non-slip and non-permeable conditions. The grid-interfaces between vanes and stator were defined as the sliding boundary condition.
Firstly, the original pump model with 4 vanes was simulated under rotation speed of 3268 RPM. For the original model, the gap between the vane tip and stator wall is 0.05mm, the radius of vane tip is 17mm, and the absolute pressures at the inlet and outlet boundary were given as 47KPa and 501KPa respectively. After comparing the calculated results and experimental results of the case, the cases with different radius of vane tip (R=34mm and 51 mm) were simulated. The influences of different radius of vane tip to performances of vane pump were analysized.

Results and Discussion

Figure 4 presents the cavitation distributions on a section of the vane pump under different rotator angle. A volume fraction 1 represents the vapor of oil while zero stands for the liquid phase and the values between 0 and 1 represent transition region of liquid oil and vapor of oil. The cavitation region in the duct of inlet is relative stable during the vane rotating while the cavitation region along the rotor is unstable, which is generated before the sealing region is closed, developed in the sealing region 1 and collapsed during the sealing region being opened. The generation, development and collapse of cavitation lead to accumulation and release of the mass of oil. The instantaneous flow rates at inlet and outlet versus rotor angle are showed in Figure 5. Corresponding to the variation of cavitation region, the instantaneous flow rates at inlet is stable while the one at outlet fluctuates significantly. For the pressure in the delivery region is higher than the value in sealing region 1, when the vane rotates from sealing region 1 to the delivery region, some lubricant oil in delivery region flows back to sealing region 1, resulting in the phenomenon of rapid decrease and subsequent recovery of flow rate at outlet. The averaged values of flow rate at inlet and outlet over a period are 36.53L/min and 37.66 L/min. When the cavitation model is involved, numerical errors are introduced in the process of dealing with the vapor/liquid interface. As a consequence, there exists the difference between inlet and outlet values of average flow rate but the mass conservation law is still satisfied in general. The averaged values of flow rate at inlet and outlet is close to flow rate obtained from experimental test, which is 38.1 L/min.

The caviatation distributions of pump with different radius of vane tip on a section depicted in

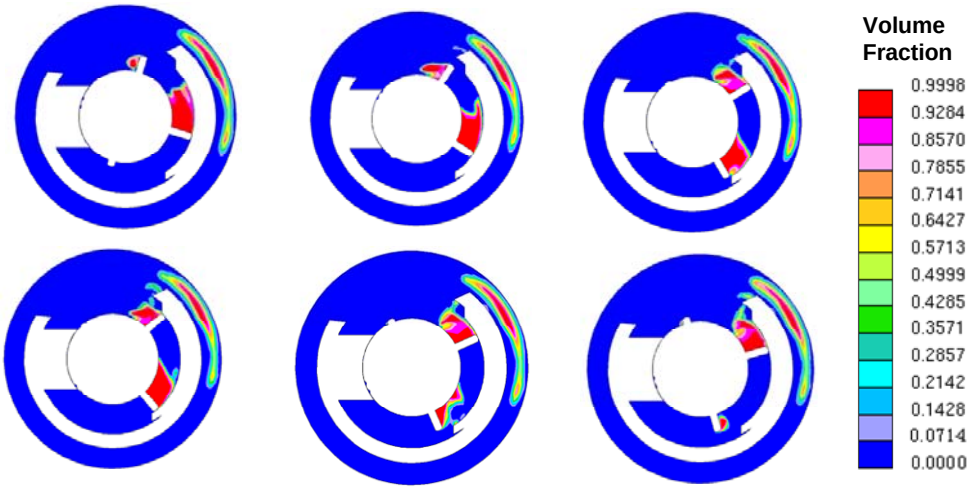

Figure 4 Cavitation distributions on a section of the vane pump

Figure 6 are presented in Figure 7. With the increase of radius of vane tip from R=17mm to R=51mm, the cavitation areas are expanded a little when the sealing region is closed. At the same rotor rotating angle, the leakage velocity from delivery region to sealing region is showed in Figure 9. Although the minimal size of the gap is the same, which is 0.05mm, the area of inlet and outlet of the gap is reduced and the

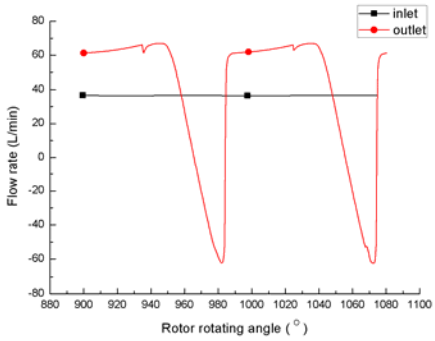

Figure 5 Instantaneous flow rates at inlet and outlet

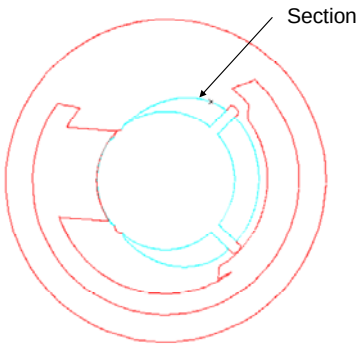

Figure 6 Section position

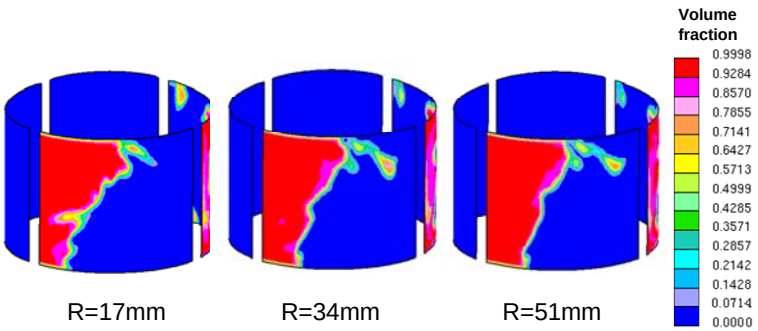

Figure 7 Cavitation distributions with different radius of vane tip

pressure loss is enhanced with increase of radius of vane tip. So the leakage velocity is somewhat larger for the case R=17mm.

Corresponding to the differences of cavition distributions and velocity magnitudes discussed above, Figure 10 shows the instantaneous flow rate during the sealing region being closed is a little larger with R=51mm while the back flow rate during the sealing region is being opened is increase slightly. The averaged flow rate of outlet is given in the Table 1 below.

Table 1 Averaged flow rate at outlet

Radius of vane tip (mm)	17	34	51
Flow rate (L/min)	37.66	36.5	36.2

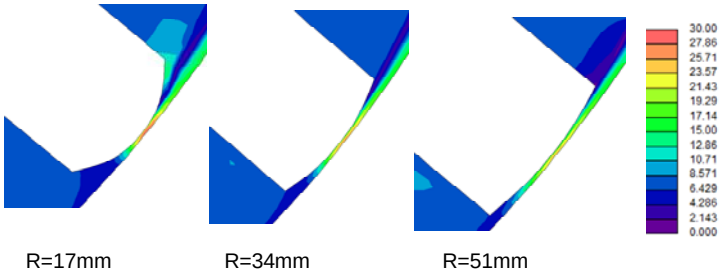

Figure 9 Leakage velocity distributions from delivery region to sealing region with different radius of vane tip

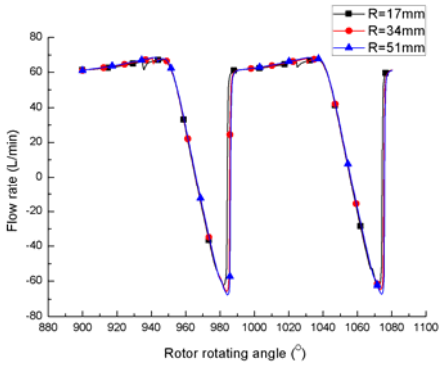

Figure 10 Instantaneous flow rates at outlet with different radius of vane tip

Conclusions

Cavitation is generated, developed and collapsed during the rotation of vane, which leads to accumulation and release of the mass of oil, corresponding to a reduced and increased area of cavitation respectively, and the transient flow rate of inlet is stable while the one at outlet fluctuates significantly. The radius of vane tip influences the cavitation area and leakage velocity during the sealing region being closed and opened; the averaged flow rate at outlet of pump over a period is a little larger in the pump with small radius of vane tip.

References

Shcherbin, V. D. and Smolyanskii, B. G. (1994) Optimization of geometry of working chamber of sliding-vane pump with circular stator, *Chemical and Petroleum Engineering,* **31,154-157.**

Cho, M. R. and Han, D. C. (1998) Vane tip detachment in a positive displacement vane pump, *KSME International Journal,* **12,881-887.**
Wu, Y.L. (2005) Fluid machinery engineering. Beijing: China Environmental Science Press.
Antonio, G. and Rosario, L. (2005) Cam shape and theoretical flow rate in balanced vane pumps, *Mechanism and Machine Theory,* **40,353-369.**
Wang, L. and Quan, L. (2006) Transient flux analysis and calculation on single-acting vane pump. *Journal of Vibration, Measurement & Diagnosis*, **26,188-191.**
Menter, F. R. (1994) Two-equation eddy-viscosity turbulence models for engineering applications, *AIAA Journal,* **32, 1598-1605.**
Ahuja,V., Hosangadi, A. and Arunajatesan, S. (2001) Simulation of cavitating flows using hybrid unstructured meshes, *Journal of Fluids Engineering,* 123,331–340.
Bakir, F., Rey, R. and Gerber, A. G. (2004) Numerical and experimental investigations of the cavitating behavior of an inducer, *International Journal of Rotating Machinery*, **10,15–25.**
Hirt, C. W. and Nichols, B. D. (1981) Volume of fluid （VOF） method for the dynamics of free boundary, *Journal of Computational Physics*, 39,201-225
Ubbink, O. And Issa, R. I.(1999) A method for capturing sharp fluid interfaces on arbitrary meshes, *Journal of Computational Physics,* 153,26-50
Demirdzic, I. and Peric, M. (1998) Space conservation law in finite volume calculations of fluid flow, *International Journal for Numerical Methods in Fluids,* 8,1037-1050.